Normal and Parallel Permeability of Preform Composite Materials used in Liquid Molding Processes: Analytical Solution

M. Nazari [*], M.M. Shahmardan , M. Khaksar , M. Khatib , S. Mosayebi

Mechanical Engineering, Shahrood University of Technology, Shahrood, Iran

ABSTRACT

The permeability of the preform composite materials used in liquid molding processes such as resin transfer molding and structural reaction injection molding is a complex function of weave pattern and packing characteristics. The development of tools for predicting permeability as a function of these parameters is of great industrial importance. Such capability would speed process design and optimization and provide a step towards establishing processing-performance relations. In this study, both normal and parallel permeability of fibrous media comprised of ordered arrays of elliptical cylinders is studied analytically. A novel scale analysis technique is employed for determining the normal permeability of arrays of elliptical fibers. In this technique, the permeability is related to the geometrical parameters such as porosity, elliptical fiber diameters, and the tortuosity of the medium. Following a unit cell approach, compact relationships are proposed for the first time for the normal permeability of the studied geometries. A comprehensive analysis is also performed to determine the permeability of ordered arrays of elliptical fibers over a wide range of porosity and fiber diameters. The developed compact relationship is successfully verified through comparison with the present results. As a result of assuming an elliptical cross section for the fibers in this analytical analysis, an extra parameter comes to play; therefore, the present analytical solution will be more complicated than those developed for circular fiber type in the literature.

© 2016 IAU, Arak Branch.All rights reserved.

Keywords : Permeability; Elliptical fibers; Fibrous media; Scale analysis; Analytical; Parametric study.

1 INTRODUCTION

F ABRICATION of fiber-reinforced plastic composites in liquid molding processes such as resin transfer molding and structural reaction injection molding involves flow in fibrous porous media. Modeling of fluid flow in liquid molding is increasingly relied upon as an efficient and cost-effective means for eliminating trial-and-error efforts in the mold design process.

The study of flow in fibrous porous media is also important in several natural and industrial areas including: thermal insulations, physiological systems, filtration and separation of particles, composite fabrication, heat exchanger design, and fuel cell technology. One can see the following references: Tomadakis and Robertson [1], Gostick et al. [2], Ismail et al. [3], Tamayol and Hooman [4] and Tamayol et al. [5].

---

[*]Corresponding author. Tel.: +98 273-3392204.
E-mail address: mnazari@shahroodut.ac.ir (M. Nazari).

Researchers have employed various theoretical and experimental techniques to predict the relationship between the pressure drop and the volumetric flow rate; comprehensive reviews of the pertinent literature can be found elsewhere; see Tomadakis and Robertson [1], Kaviany [6] and Yazdchi and Luding [7].

Experimental observations indicated a linear relationship between the volume-averaged superficial fluid velocity, U_D, and the pressure gradient [6]:

$$-\frac{dP}{dx} = \frac{\mu}{K}U_D \qquad (1)$$

where, μ is the fluid viscosity and K is the permeability of the medium. Eq. (1), Darcy's equation, holds when flow is in creeping regime. Permeability of a porous medium is related to its geometrical parameters including: porosity, particles shape, pore distribution, particles arrangement, and orientation.

Based on the orientation of fibers in the space, fibrous materials can be divided into 1, 2, and 3 directional media as mentioned by Tomadakis and Robertson [1] and Tamayol et al. [5].   In one-directional (1D) structures the axes of fibers are parallel to each other. In two directional (2D) fibrous matrices the fibers axes are located on planes parallel to each other with random positions and orientations on these planes. The axes of fibers in three-directional (3D) are randomly positioned and oriented in space. The simplest representation of fibrous media is an ordered 1D structure in the form of an array of parallel fibers. 1D structures have been considered by researcher for developing analytical or semi-analytical models for permeability of fibrous media. It is noteworthy that the permeability of random 2D and 3D media can be related to the values for 1D structures. Many researchers such as Jackson and James [8], Tamayol and Bahrami [9], Mattern and Deen [10] and Happel [11] indicated this matter.   Thus, the permeability of 1D structures are investigated in the present study.

Pioneering experimental and theoretical studies for determining the permeability of fibrous started in 1940s (Carman [12], Sullivan [13]). Later, Sparrow and Loeffler [14] and Hasimoto [15] used series solutions for estimating the permeability of ordered arrangement of cylinders. Kuwabara [16] solved stream function and vorticity transport equations and employed a limited boundary layer approach to predict the permeability of flow normal to randomly arranged fibers for materials with high porosities. Happel [11] analytically solved the Stokes equation for parallel and normal flow to a single cylinder with free surface model. He assumed that the flow resistance of a random 3D fibrous structure is equal to two third of the normal flow resistances of 1D array of cylinders plus one third of the parallel. Sangani and Acrivos [17] performed analytical and numerical studies on viscous permeability of square and staggered arrays of cylinders, when their axes were perpendicular to the flow direction. Their analytical models were agreement with the lower and higher limits of porosity. Drummond and Tahir [18] solved Stokes equations for normal and parallel flow towards different ordered structures. They used a distributed singularities method to find the flow-field in square, triangular, hexagonal and rectangular arrays. However, their proposed model for normal permeability of arrays of circular cylinders had a limited range of accuracy. Hellou et al. [19] theoretically predicted the permeability of general triangular arrays of fibers. They also proposed a correlation for determination of permeability of periodic triangular arrangements.

Tamayol and Bahrami [20] extended the lubrication theory approach proposed by Gebart [21] and studied permeability of touching and non-touching ordered fibrous media towards normal and parallel flow. Analytical models were developed using the concept of "unit cell" and introducing an "integral technique". They reported compact analytical relationships for pressure drop and permeability of square arrays of cylindrical fibers.

Numerical studies cover a wider range of fibrous media in terms of porosity and fiber orientation and are more frequent in the literature, see for example: Westhuizen and Plessis [22], Sahraoui and Kaviany [23], Sobera and Kleijn [24], Clague and Phillips [25], Nabovati et al. [26] and Higdon and Ford [27].

Dahua Shou et al. [28] theoretically studied transverse flow through aligned yarns with two length scales. They calculated the permeability as a function of porosity, fiber radius, fiber cross-sectional shape, and fiber packing design. Dahua Shou et al. [29] also theoretically investigated the permeability of aligned fiber arrays from ordered configuration to random pattern, based on a geometrical scaling rule. Xiaohu Yang et al. [30] demonstrated that the permeability of isotropic porous media, e.g. open-cell foams, can be analytically presented as a function of two morphological parameters: porosity and pore size. Dahua Shou et al. [31] theoretically studied the longitudinal permeability of the packed fibers.

In a notable study, Sobera and Kleijn [24] recently analytically and numerically studied the permeability of random 1D and 2D fibrous media. The comparison of the model of Sobera and Kleijn [24], which was an extension of the analysis proposed by Clague and Phillips [25], with their numerical results revealed that their model was only accurate in highly porous materials. Recently, Tamayol and Bahrami [9] modified the model of Sobera and Kleijn

[24] by introducing the tortuosity of the porous medium in their scale analysis. The model of Tamayol and Bahrami [9] showed a good agreement with the numerical and experimental data collected from various sources for 1D, 2D, and 3D structures. However, the accuracy of this model for non-circular fibers was not investigated.

Our literature review showed that despite numerous studies aiming at determining the permeability of fibrous media, less attention has been paid to determination of permeability of non-cylindrical fibers. The majority of the existing models and techniques are not general and fail to predict the permeability over the entire range of porosity and fiber shape. Thus, here we want to develop an analytical approach that is applicable to 1D elliptical fibrous structures. The scale analysis technique is also followed for determining the normal permeability of elliptical fibers in square and staggered arrangements. The permeability is related to the porosity, elliptical fiber diameters, and the tortuosity of the medium. Due to lack of experimental and numerical data for permeability of non-circular fibers, an independent numerical analysis is carried out over a wide range of porosity and fiber diameter ratio; the results are used to validate the developed compact relationship. The developed solutions are successfully compared with analytical and numerical results.

2   MODELING APPROACH

2.1 Problem statement

In the present study, the 1D fibrous media comprised of arrays of elliptical fibers in staggered and square arrangements are studied. To simplify the analysis, by neglecting the entrance and exit effects, a unit cell approach is followed. The unit cells, shown in Fig. 1, are the smallest volumes which can represent the characteristics of the whole microstructure. Here, the fibers are considered long enough to neglect the variations in the *z*-direction, although the velocity distribution in porous material in fact is 3D. Porosity for the arrangement can be determined

from: $\varepsilon = 1 - \dfrac{\pi dD}{4S^2}$; *Square*

$$\varepsilon = 1 - \dfrac{\pi dD}{4S_x S_y} ; \quad Staggered \tag{2}$$

and the solid volume fraction defined,

$$\varphi = 1 - \varepsilon \tag{3}$$

where D, d and S are the major diameter of ellipse, the minor fiber diameter, and the distance between the centers of two adjacent fibers, respectively. Darcy's equation Eq. (1) holds when flow is in creeping regime and the inertial effects are negligible in this regime. Here, the flow is assumed to be steady state, incompressible and porous media is completely saturated. Therefore, the pore-scale velocity is governed by Stokes equation (in the creeping regime):

$$\nabla \vec{V} = 0 \tag{4}$$

$$\mu \nabla^2 \vec{V} = -\nabla P \tag{5}$$

2.2 Scale analysis model development

In the scale analysis approach, the scale or the range of variation of the parameters is substituted in governing equations. Moreover, the derivatives in the governing equations are approximated with differences, see White [32]. Following Tamayol and Bahrami [9] and Tamayol et al. [5], Sobera and Kleijn [24] and Clague et al. [25], half of the minimum opening between two adjacent ellipses, δ_{min}, is selected as the characteristic length scale over which rapid changes of the velocity occurs.

Tamayol and Bahrami [9] employed the Carman's hypothesis stating that a fluid particle to path through a sample of size L should travel in a tortuous path of length L_e. They argued that the pore-level velocity scale is inversely related to L_e / L (when a constant pressure difference applies). This ratio is called tortuosity factor, τ. Following this assumption, they suggested the following pore-level velocity scale which is adopted in the present analysis:

$$\left|\vec{V}\right| \sim \frac{U_D}{\tau\beta} \tag{6}$$

where β is the ratio of minimum to total frontal areas. Substituting from Eq. (6) for velocity scale and using δ_{min} as the length scale, permeability can be calculated as:

$$\frac{\mu}{K}U_D \approx \mu \frac{U_D}{\tau\beta\delta_{min}{}^2} \Rightarrow K = C\beta\delta_{min}{}^2\tau, \beta = \frac{\delta_{min}}{S} \tag{7}$$

where C is a constant that should be determined through comparison with experimental or numerical data. Therefore, one needs to know the ratio between tortuosity factor, τ, and minimum to total frontal area, β, to calculate the permeability. The ratio of the average distance, L_e, that a particle should travel to cover a direct distance of L called tortuosity factor. Because of its importance in mass and thermal diffusion, several empirical and theoretical relationships have been proposed for tortuosity calculation in the literature; good reviews can be found elsewhere: Archie [33] and Shen and Chen [34]. The Archie's law (in 1942) is one of the most popular empirical models for determination of tortuosity which is used in the present analysis:

$$\tau = \left(\frac{1}{\varepsilon}\right)^{\alpha} = \left(\frac{1}{1-\varphi}\right)^{\alpha} \tag{8}$$

where ε is the porosity and α is a constant. Tamayol and Bahrami [9] Showed that $\alpha = 0.5$ provides a good estimate for the tortuosity of ordered arrays of circular fibers. Here α is assumed to be equal to 0.5.

2.3 Numerical Analysis

The flow Reynolds number in the numerical simulations should be kept sufficiently low to ensure negligible effects of inertial terms. Therefore, to guarantee that creeping flow exists, the inlet velocity is set low enough, which the Reynolds number based on the fibers diameter, d, is below 0.05 for all cases.

2.3.1 Cross flow permeability

In this paper, the results of the "Cross Flow" permeability are reported in the case of fully-developed flow. It means that the volume averaged velocity does not change in the consecutive unit cells, in the fully developed region. Therefore, suitable boundary conditions should be considered for the numerical analysis of fluid flow through a unit cell. Inlet and outlet boundaries of a fully developed cell should be considered as periodic boundaries. The pressure gradient, i.e. $\Delta P/S$, is the same for the unit cells that are located in the fully developed section. Another way to simulate the fluid flow through the unit cell is consideration of a set of 7-10 unit cells in series. The selected series geometries have to be arranged in a way that the fully developed condition is reached. The velocity profiles are compared at the entrance to each unit cell. In other word, the unit cells which are located far from the inlet can be considered as fully developed cells. The inlet velocity of the media is assumed to be uniform and velocity inlet boundary condition is applied. The normal gradient of properties along the outlet is zero and the values of all properties at the outlet are interpolated from the computational domain. The symmetry boundary condition is applied on the side borders of the considered unit cells; this means that normal velocity and gradient of parallel component of the velocity on the side borders are zero. The Finite volume method is used for solving the governing equations and SIMPLE algorithm is selected for pressure-velocity coupling. Second order upwind scheme is also employed to discrete the governing equations, see Versteeg and Malalasekera [35]. Different numerical grids are employed to check the grid independency of the results. The number of grids (in a periodic square unit cell) is listed in the Table 1. , for a given porosity. More descriptions about the numerical results will be provided in Sec. 3.1.

2.3.2 Parallel flow permeability

The same unit cell used is used for numerical simulation of the creeping flow ''Parallel'' to arrays of elliptical cylinders. For convenience and without loss of generality, only the square arrangement of elliptical fibers is studied numerically. Since the analytical solutions for permeability are reported for fully developed flow, the length of the cylinders in the computational domain is assumed to be 40 times the major radius since in this length velocity profile is fully developed and the unit cell result considered in fully developed velocity profile. A finite volume method is also used for solving the governing equations and SIMPLE algorithm is selected for pressure-velocity coupling. Second order upwind scheme is employed to discrete the governing equations. Creeping flow regime results in fast development of velocity profile. The inlet velocity of the media is assumed to be uniform and velocity inlet boundary condition is applied. The normal velocity and the gradient of parallel component of the velocity on the side borders are zero. Therefore, the symmetry boundary condition is applied on the side borders of the unit cells. For decreasing the time of computations, just a quarter of cell is used for numerical simulation.

3 RESULTS AND DISCUSSION

Eq. (7) defined the permeability of fibrous media related to the minimum opening between adjacent fibers, δ_{min}, ratio between minimum to total frontal area, β, and tortuosity factor, τ. The tortuosity factor can be calculated from Eq. (8). In the following sections, C will be calculated using geometrical properties and numerical analysis. The permeability is then related to the solid volume fraction. In the following subsections, our focus will be on the pressure drop and permeability for the flow through presented fibrous structure.

3.1 Numerical results

Once the pressure drop is known, permeability can be calculated from Eq. (1). In this equation, the pressure drops are the values obtained from the analysis of fully developed unit cells. As presented in Sec. 2.3, a set of 7-10 unit cells (in series) is considered as computational domain for the case of cross flow. The selected series geometries have to be arranged so that the fully developed condition is reached. The velocity profiles are compared at the entrance to each unit cell and those with fully-developed velocity profile are considered in the analysis

The predicted values for the non-dimensional permeability, i.e. $K^*=K/dD$, volume averaged velocity in the cell, and the pressure loss across one unit cell (in the case of normal flow) are reported in Table 1. , considering different configurations used in the numerical analysis (related to square arrangement of fibers). The inlet velocity is set low enough to guarantee that creeping flow exists. The Reynolds number based on the fibers minor diameter, d, is below 0.05 for all cases. For specific values of the major and minor diameters, D and d, the porosity of the unit cell is a function of the distance between two adjacent fibers, S.

Numerical results are also obtained from a 3D analysis of parallel flow through elliptical fibers. To check the grid independency of the obtained results, different number of grids are employed, which for brevity are not presented here. The permeability can be calculated from Eq. (1). By calculation of the pressure drop in the porous structure, the permeability can be evaluated from this relation. A constant, uniform inlet velocity is considered for all test cases; therefore, the volume averaged and the inlet velocities for parallel flows are related as:

$$U_D = u_{inlet} \times \varepsilon \tag{9}$$

Using the values of the pressure drop obtained from the numerical simulations, the calculated values of parallel permeability are listed in Table 2.

3.2 Scale analysis
3.2.1 Square arrangement

For the ordered 1D unit cell shown in Fig.1(a), it can be seen that $\beta = (S - d)/S$ and $\delta_{min} = (S - d)$. Therefore, Eq. (7) can be rewritten as:

$$K = C \frac{(S-d)^3}{S\sqrt{1-\varphi}} \tag{10}$$

The values of normal flow permeability versus porosity were reported in Table 1. using the numerical finite volume approach. By comparing the numerical results (for a wide range of porosity and fiber diameter ratio, $\omega = D/d$) with the presented model, i.e. Eq. (10), it was noticed that the constant parameter of C=0.133 captures the trend of the numerical data over the entire range of porosity and fiber diameter ratio. Therefore, the following relationship is suggested for calculating the dimensionless permeability of the ordered structures,

$$K^* = \frac{K}{dD} = 0.133 \frac{(S-d)^3}{dDS\sqrt{1-\varphi}} \tag{11}$$

Using Eqs. (2) and (3), after some mathematical manipulations, one can write,

$$K^* = \frac{0.133\left[\frac{\pi}{4\varphi} - 3\sqrt{\frac{\pi}{4\omega\varphi}} + \frac{3}{\omega} - \sqrt{\frac{4\varphi}{\omega^3\pi}}\right]}{\sqrt{1-\varphi}} \tag{12}$$

It should be noted that Eq. (12) captures the trend of numerical results over the entire range of porosity and fiber diameter ratio. However, in favor of brevity, only the numerical results for a specific case of $D = 1.4$ cm, $d = 1$ cm is listed in Table 1. A comparison of the present results and several existing models is plotted in Fig. 2 and the rusults are compared with experimental data found in the literature; such as Tamayol and Bahrami [9], Bergelin et al. [36], Chmielewski and Jayaraman [37], Khomami and Moreno [38], Kirsch and Fuchs [39], Sadiq et al. [40] and Zhong et al. [41], for the case of fluid flow through circular fibers, i.e., $\omega = 1$. All of the models could capture trends of data in higher limits of porosity. The presented model predicts the trends of data accurately over the entire range of porosity.

Table 1
The numerical results of normal permeability of square arrangement, D=1.4(cm), d=1(cm) and u_{inlet}=0.05(m/s).

ε	No. of Grids in a Unit Cell	S (cm)	U_D (m/s)	ΔP (Pa)	K^*
0.51	1223	1.489	0.0166	18.7	0.00902347
0.72	1859	1.982	0.02477	7	0.04765776
0.79	2619	2.290	0.02817	4.79	0.091385
0.86	4292	2.804	0.03217	3.023	0.2024694
0.91	5921	3.496	0.0357	1.937	0.4372
0.96	6352	5.26	0.0405	0.93	1.554136
0.989	6784	10	0.045	0.34	8.98109

Table 2
The numerical results of parallel permeability, $a = 0.7$(cm), $b = 0.5$(cm) and $u_{inlet} = 0.05$(m/s).

ε	S(cm)	L(cm)	UD(m/s)	ΔP(Pa)	K*	Reynolds number
0.51	1.489	4	0.0255	58.269	0.0138	0.009
0.63	1.724	4	0.0315	29.523	0.0335	0.01
0.79	2.290	5	0.0396	10.8391	0.1435	0.013
0.86	2.804	5	0.0430	5.0355	0.3355	0.016
0.96	5.260	5	0.0480	0.66515	2.835	0.03

3.2.2 Staggered arrangement

Using the geometrical properties of the unit cells shown in Figs. 1(b) and 3, one can write:

$$\delta_{min}{}^2 = m^2 + n^2 \tag{13}$$

where m and n can be defined as:

$$n = \frac{S_x}{2} - 2\left(\frac{4}{D^2} + \frac{16}{d^2}\left(\frac{S_y}{S_x}\right)^2\right)^{(-\frac{1}{2})} \quad ; m = S_y - 2\left(\frac{1}{D^2}\left(\frac{S_x}{S_y}\right)^2 + \frac{4}{d^2}\right)^{(-\frac{1}{2})} \tag{14}$$

In the above definition, r and z can be defined as:

$$r = \left(\frac{4}{D^2} + \frac{16}{d^2}\left(\frac{S_y}{S_x}\right)^2\right)^{(-\frac{1}{2})} \qquad z = \frac{S_y}{S_x/2}r \;\rightarrow\; z = \left(\frac{1}{D^2}\left(\frac{S_x}{S_y}\right)^2 + \frac{4}{d^2}\right)^{(-\frac{1}{2})} \tag{15}$$

Therefore, δ_{min} can be calculated as below:

$$\begin{aligned}
\delta_{min}{}^2 = S_y{}^2 &+ 4\left(\frac{1}{D^2}\left(\frac{S_x}{S_y}\right)^2 + \frac{4}{d^2}\right)^{(-1)} - 4S_y\left(\frac{1}{D^2}\left(\frac{S_x}{S_y}\right)^2 + \frac{4}{d^2}\right)^{(-\frac{1}{2})} \\
&+ \frac{S_x{}^2}{4} + \left(\frac{1}{D^2} + \frac{4}{d^2}\left(\frac{S_y}{S_x}\right)^2\right)^{(-1)} - S_x\left(\frac{1}{D^2} + \frac{4}{d^2}\left(\frac{S_y}{S_x}\right)^2\right)^{(-\frac{1}{2})}
\end{aligned} \tag{16}$$

Employing the following dimensionless parameters:

$$a = \frac{S_x}{D}, b = \frac{S_y}{D}, \omega = \frac{D}{d} \tag{17}$$

The dimensionless form of Eq. (16) can be expressed as follows:

$$\frac{\delta_{min}}{D} = \left[b^2 + 4\left(\frac{a^2}{b^2} + 4\omega^2\right)^{-1} - 4b\left(\frac{a^2}{b^2} + 4\omega^2\right)^{-\frac{1}{2}} + \frac{a^2}{4} + \left(1 + \frac{4\omega^2 b^2}{a^2}\right)^{-1} - a\left(1 + \frac{4\omega^2 b^2}{a^2}\right)^{-\frac{1}{2}} \right]^{\frac{1}{2}} \tag{18}$$

Using the dimensionless parameters defined in Eq. (18), the porosity and the tortuosity becomes:

$$\varepsilon = 1 - \frac{\pi dD}{4S_x S_y} = 1 - \frac{\pi}{4ab\omega} \tag{19}$$

$$\tau = \left(\frac{1}{\varepsilon}\right)^{0.5} = \left(\frac{4ab\omega}{4ab\omega - \pi}\right)^{0.5} \tag{20}$$

Similarly, the ratio of the minimum to the total frontal area, β, becomes:

$$\beta = \frac{\delta_{min}}{\sqrt{\left(\dfrac{S_x}{2}\right)^2 + S_y{}^2}} = \frac{\dfrac{\delta_{min}}{D}}{\sqrt{\left(\dfrac{a}{2}\right)^2 + b^2}} \tag{21}$$

The dimensionless normal permeability of elliptical cylinders in staggered arrangements become:

$$K^* = \frac{K}{D^2} = \frac{C}{\sqrt{\left(\frac{a}{2}\right)^2 + b^2}} \left[\begin{array}{c} b^2 + 4\left(\frac{a^2}{b^2} + 4\omega^2\right)^{-1} - 4b\left(\frac{a^2}{b^2} + 4\omega^2\right)^{-\frac{1}{2}} \\ + \frac{a^2}{4} + \left(1 + \frac{4\omega^2 b^2}{a^2}\right)^{-1} - a\left(1 + \frac{4\omega^2 b^2}{a^2}\right)^{-\frac{1}{2}} \end{array} \right]^{\frac{3}{2}} \left(\frac{4ab\omega}{4ab\omega - \pi}\right)^{\frac{1}{2}} \tag{22a}$$

And for a simple case of $S_x = S_y = S$, one would have,

$$K^* = \frac{4C}{\sqrt{5\frac{\pi}{\omega\varphi}}} \left[\frac{5}{16}\frac{\pi}{\omega\varphi} + 5\left(1 + 4\omega^2\right)^{-1} - \frac{5}{2}\sqrt{\frac{\pi}{\omega\varphi}}\left(1 + 4\omega^2\right)^{-\frac{1}{2}} \right]^{\frac{3}{2}} \left(\frac{1}{1-\varphi}\right)^{\frac{1}{2}} \tag{22b}$$

Eq.(22) shows that the permeability as a function of dimensionless geometry parameters a, b, ω. The proportionality coefficient *C*, should be determined through comparison of Eq. (22) with experimental or numerical data in a way that the least deviation can be achieved. The comparison of the numerical data and the proposed model suggests that Eq. (22) with C =0.0827 can predict the trend of the numerical results. It should be noted that if a constant value is selected for C, the model can only qualitatively predict the data. Table 3. shows the comparison of the values obtained from Eq. (22) with those calculated from the numerical approach for *D/d* = 1.1, 1.4; according to the table, the presented differences between numerical and analytical solutions are acceptable. In Fig. 4, the predicted results of Eq. (22) for staggered arrangement of circular fibers are compared with existing experimental data, i.e.Tamayol and Bahrami [9], numerical results of Higdon and Ford [27] and Hellou et al. [19]. It can be seen that the proposed model can predict the trend of numerical and experimental results over the entire range of porosity.

Table 3
Comparison of the results of the Eq. (22) with numerical results, for two different values of D/d..

D/d=1.1			Relative Error	D/d=1.4			Relative Error
ε	$(K/D^2)_{Eq.(22)}$	$(K/D^2)_{Num.}$		ε	$(K/D^2)_{Eq.(22)}$	$(K/D^2)_{Num.}$	
0.286	0.000913	0.000916	0.32%	0.570	0.01123	0.01182	5%
0.400	0.002639	0.002630	0.34%	0.619	0.01670	0.01685	0.89%
0.559	0.009812	0.009857	0.45%	0.809	0.08089	0.08404	3.7%
0.662	0.023066	0.023134	0.29%	0.859	0.14650	0.15103	3%
0.733	0.043430	0.043292	0.32%	0.892	0.23783	0.24172	1.6%
0.904	0.342061	0.342608	0.16%	0.952	0.87773	0.87471	0.34%
-	-	-		0.979	2.85545	2.98676	4.4%

3.3 Analytical solution for parallel flow permeability

Following previous studies on pore-level analysis of transport phenomena in porous media, a unit cell approach is followed for determining the parallel permeability of unidirectional arrays of elliptical fibers. The unit cell (or basic cell) is defined the smallest volume which can represent the characteristics of the whole microstructure. Porous media are assumed to be periodic and the unit cells repeat throughout the material. The unit cells are selected as the space between adjacent elliptical cylinders, as shown in Fig. 1, where the fluid flow is perpendicular to paper. Without affecting the generality of the analysis, in the following derivations, it is assumed that $S_x = S_y = S$. It should be noted that the analysis can be rewritten for the general case. Assuming creeping, constant properties, and incompressible flow, the *z*-momentum equation reduces to stokes equation. The unit cell is divided into two regions, and two different velocity distributions are considered. Due to symmetry, it is sufficient to consider the flow in the region defined by $x = 0$ to $x = S/2$ and $y = 0$ to $y = -S/2$. No-slip boundary conditions valid for the first interval $0 < x < a$ whereas this condition is not reliable for the other region in the unit cell. Actually, the flow at the region $a < x < S/2$ is similar to flow between two parallel surfaces which are moving in *z*-direction. The half thickness of the unit cell in y-direction is defined δ. For the rectangular arrangement, the thickness of unit cell is presented as:

$$\delta = \begin{cases} \dfrac{S}{2} - \sqrt{b^2 - \dfrac{b^2 x^2}{a^2}} & 0 \le x \le a \\[4mm] \dfrac{S}{2} & a \le x \le \dfrac{S}{2} \end{cases} \tag{23}$$

By assuming that the fluid flow at $y = \pm S/2$ is similar to flow between two fixed parallel surfaces, the boundary conditions for $a < x < S/2$ and $y = \pm S/2$ can be written as:

$$w(x) = -\frac{1}{2\mu}\frac{dP}{dz}[x^2 - Sx + aS - a^2] \tag{24}$$

The velocity profile for this interval is as follows:

$$w(x,y) = -\frac{1}{2\mu}\frac{dP}{dz}[y^2 + x^2 - Sx + aS - a^2 - \frac{S^2}{4}], \quad a < x < S/2 \tag{25}$$

After some manipulations, Eq. (25) for the presented unit cell becomes:

$$w(x,y) = \begin{cases} -\dfrac{1}{2\mu}\dfrac{dP}{dz}(\delta^2 - y^2) = w_1 & 0 \le x \le a \\[4mm] -\dfrac{1}{2\mu}\dfrac{dP}{dz}(\dfrac{S^2}{4} - (x - \dfrac{S}{2})^2 + (a - \dfrac{S}{2})^2 - y^2) = w_2 & a \le x \le \dfrac{S}{2} \end{cases} \tag{26}$$

where Eq. (26) is a parabolic velocity profile and δ is calculated from Eq. (23). Using the continuity equation, one can calculate the volumetric flow rate through the unit cell as:

$$Q = \iint\limits_{unit\ cell} w(x,y)\,dy\,dx = \iint w_1\,dy\,dx + \int w_2\,dy\,dx \tag{27}$$

where,

$$Q_1 = \int_0^a \int_{-(\frac{S}{2} - b\sqrt{1 - x^2/a^2})}^{(\frac{S}{2} - b\sqrt{1 - x^2/a^2})} \left(\frac{1}{2\mu}\frac{dP}{dz}\right)\left((\frac{S}{2} - \sqrt{b^2 - (\frac{bx}{a})^2})^2 - y^2\right) dy\,dx \tag{28}$$

$$Q_2 = \int_a^{S/2} \int_{-S/2}^{S/2} \left(\frac{1}{2\mu}\frac{dP}{dz}\right)\left(\frac{S^2}{4} + (a - \frac{S}{2})^2 - (x - \frac{S}{2})^2 - y^2\right) dy\,dx \tag{29}$$

After calculation of these integrals, we will have:

$$Q_1 = -\left(\frac{1}{24\mu}\frac{dP}{dz}\right)[16Sb^2 - 3S^2 b\pi + 2S^3 - 3b^3\pi].a \tag{30}$$

$$Q_2 = -\left(\frac{1}{2\mu}\frac{dP}{dz}\right)[\frac{1}{6}S^4 - \frac{2}{3}aS^3 + a^2 S^2 - \frac{2}{3}a^3 S] \tag{31}$$

where Q_1 and Q_2 are volumetric flow rate in region 1, $0 \leq x \leq a$, and region 2, $a \leq x \leq S/2$, respectively. Using Darcy's law and substituting for Q from Eqs. (30) and (31), one can find the parallel permeability of elliptical unit cell,

$$K^* = -\frac{1}{48}\frac{1-\varphi}{\varphi a \pi b^2}\left\{ \begin{array}{l} -8\left(-\frac{3}{4}\pi^{3/2}ba - \sqrt{\pi}(-2b^2+a^2)\varphi\right)\varphi\sqrt{\frac{ab}{\varphi}} + \\ 12b\left(\frac{1}{4}\varphi^2b^2 - \frac{1}{4}a\pi(\frac{2}{3}-\varphi)b - a^2\varphi\right)\pi \end{array} \right\} \tag{32}$$

where $\varphi = 1-\varepsilon$ and $K^* = K/(4ab)$ is the non-dimensional permeability. In Fig. 5, the predicted results of Eq. (32) for staggered arrangement of circular fibers are compared with existing data. Fig. 5 shows the comparison of parallel permeability of square arrangement, between the present model, i.e. Eq. (32), and analytical model of Tamayol and Bahrami [20] and Happel [11], experimental and numerical data of Skartsis et al. [42], Sangani and Yao [43] and Tamayol and Bahrami [44]. It can be seen that the proposed model can predict the trend of numerical and experimental results over the entire range of porosity.
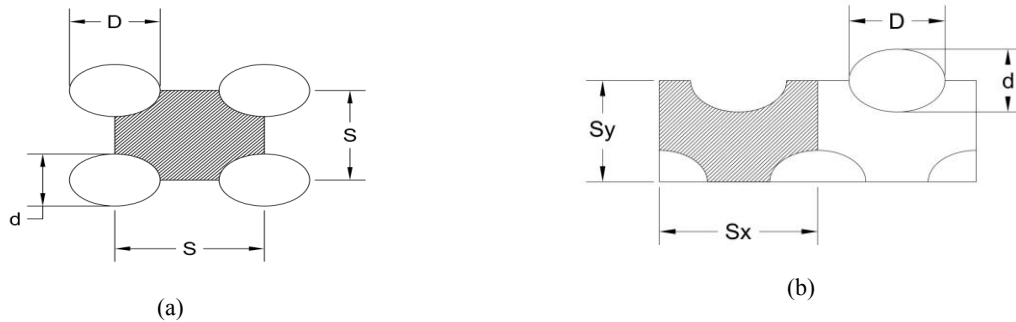

Fig.1
The unit cell considered for calculating the permeability of arrays of elliptical fibers. a) Square arrangements, b) Staggered arrangements.
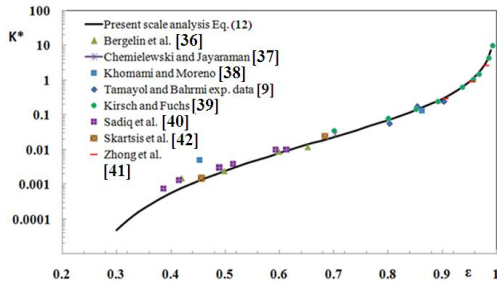

Fig.2
Comparison of the scale analysis model of Square arrangement, Eq. (12), with the existing literature (for ω=1).
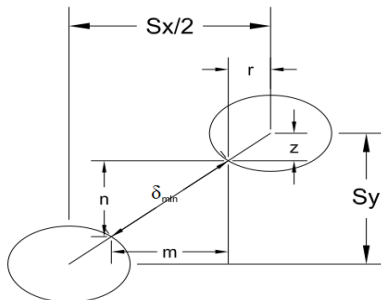

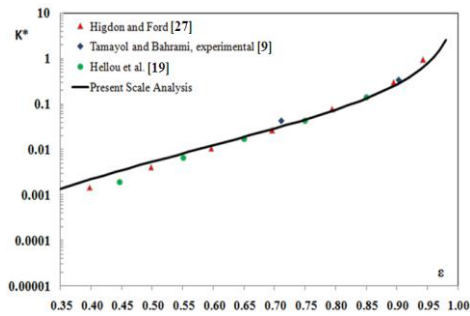**Fig.3**
Geometrical parameters for the staggered arrangement.

Fig.4
Comparison of the scale analysis model of Staggered arrangement, Eq. (22), with the existing literature (for ω=1).
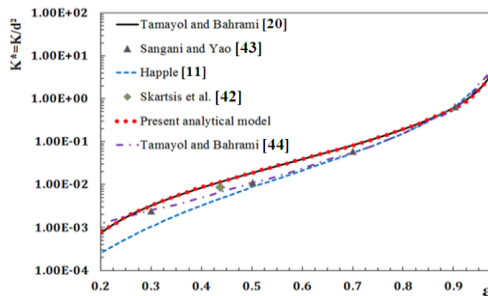

Fig.5
Comparison between present model, experimental data and analytical models in the case of parallel flow permeability.

3.4 Parametric study

Once the proposed models are validated, we can use them for performing a parametric study. The effects of fiber diameter ratio on the permeability for both arrangements are investigated and are plotted in Fig. 6 over a range of porosity. As expected, the permeability of the studied structures has a direct relationship with their porosity, ε. Moreover, the fiber diameter ratio, ω, is an important parameter in the calculation of the permeability. Increasing the diameter ratio results in permeability enhancement; especially, for the case of square arrangement of elliptical fibers. It should be noted that for square arrangements in the limiting case of $\omega \rightarrow \infty$, the problem can be treated as flow between interrupted parallel plates that yield a higher pressure drop in comparison with the case of flow through elliptical fibers. In addition, a comparison between Figs. 6(a) and (b) indicates that elliptical fibers in staggered arrangement are more permeable than those in square arrangement with the same ω and ε. The presented analytical solution can be suitability applied to flow parallel to square arrays of circular cylinders and $\omega = 1$ should be used in Eq. (32). The present model is accurate for a wide range of porosity. It is important to note that the previous models have been limited to circular cylinders and cannot be applied to media formed by non-circular fibers. Fig. 7 shows the variation of non-dimensional permeability versus porosity of unit cell, for different radius-ratio of fibers, i.e. $\omega = a/b$. It is important to notice that for each value of radius-ratio of elliptical fiber, there is a minimum value for porosity to avoid the overlapping of elliptical fibers which is mentioned in Fig. 7. According to the Fig. 7, the parallel permeability has a reverse relationship with ω, but the variation of permeability with ω is not significant specially in high porosities. As presented in Eq. (32), the parallel permeability of elliptical fibers was obtained in the case of unit aspect ratio, i.e. S_x/S_y=1. The effect of aspect ratio can be considered in non-dimensional parallel permeability as follows,

$$K^* = \frac{K}{4ab\gamma}$$

(33)

where $\gamma=S_x/S_y$ is aspect ratio. The results obtained for different aspect ratios and porosities in the case of parallel flow through a rectangular array of cylindrical fibers are shown in Fig. 8. It can be seen that the changes of parallel permeability due to the variation of aspect ratio are not significant, especially for large values of porosity. As shown in Fig. 8, there are reasonable range for both porosity and aspect ratio to avoid overlapping of adjacent fibers. In other word, the mentioned parameters are selected such that the adjacent ellipses do not overlap each others. Therefore, for a constant value of S_x/S_y, the porosity of the unit cell should be larger than a specific value. In the

case of fluid flow through circular fibers, the parallel permeability is a function of aspect ratio and porosity, whereas for elliptical cross section, another variable, i.e. radius ratio of fiber, is appeared in the permeability equations. Fig. 9 shows the variations of non-dimensional permeability versus porosity for different aspect ratios. The radius ratio, i.e. *a/b*, is considered constant in this figure. It's clear that, the aspect ratios is an important parameter affecting the parallel permeability. In other word, in the case of fluid flow through elliptical fibers, the parallel permeability depends on three parameters, 1- porosity (ε), 2- aspect ratio (S_x/S_y), and 3- radius-ratio (*a/b*).
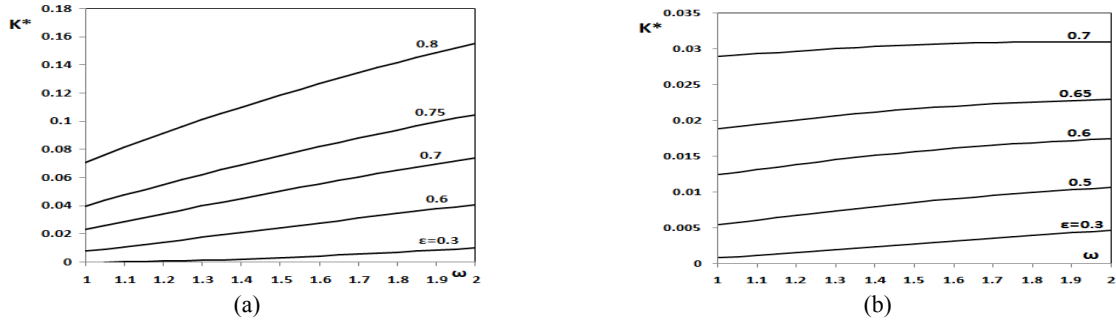

Fig.6
Permeability for different values of ω and porosity, a) Square arrangement, b) Staggered arrangement.
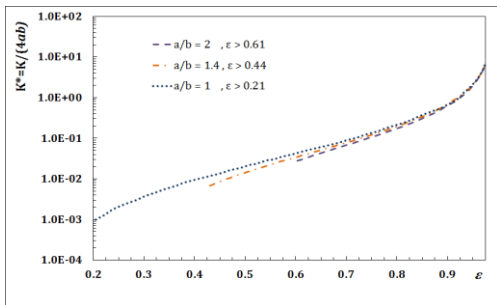

Fig.7
Non-dimensional permeability versus porosity, for different radius-ratio in parallel flow through a unit cell with elliptical cross section of fibers.
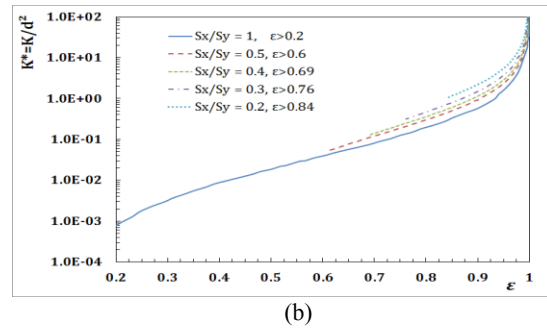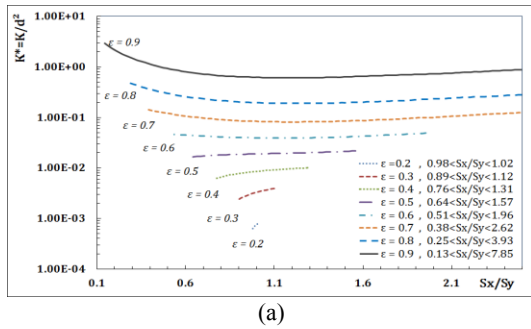

Fig.8
The variations of non-dimensional permeability versus (a) aspect ratio and (b) porosity, for parallel flow in a rectangular array of cylindrical fibers with circular cross section.
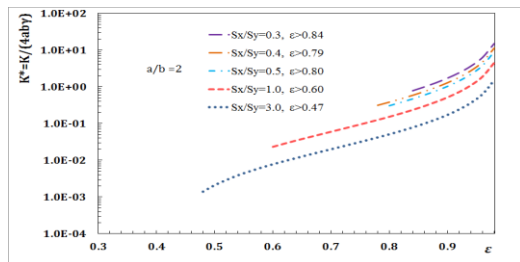

Fig.9
Non-dimensional permeability versus unit cell porosity for different values of $\gamma = S_x/S_y$.

4   CONCLUSIONS

Scale analysis technique and numerical method were employed for analyzing pressure drop and permeability of arrays of elliptical fibers in square and staggered arrangements. The fibrous structure was represented by a unit cell which was assumed to be repeated throughout the media. A closed form relation was presented for the non-dimensional permeability (as a function of porosity) using the scale analysis technique. The presented relation will be applicable for wide range of porosities. The fiber diameter ratio (for elliptical cross-section) had a significant effect on the dimensionless permeability of arrays of elliptical fibers especially at small porosities. The obtained results were compared with several existing models for the limiting case of fluid flow through circular fibers. The presented model predicts the trends of data accurately over the entire range of porosity. The reported relationships are powerful tool for analysis of flow in fibrous media made up of non-circular fibers. In this paper, the parallel flow through fibrous porous media formed by elliptical fiber in rectangular arrangements was also studied analytically. The proposed analytical model was successfully compared with analytical, experimental and numerical data available in the literatures for square arrays of circular fibers. The model was then used to investigate effects of various parameters. The highlights of this parametric study were:

- Permeability has a direct relationship with porosity and ω, but the variation of permeability with ω is not significant especially in high porosities.
- The unit cell aspect ratio affects the permeability and in highly porous structures has a direct relationship with the parallel permeability.

The present analysis provides a detailed knowledge on the effects of elliptical geometrical parameters on the permeability of fibrous media. This information can be used as guidelines and criteria to design, select, and optimize engineering systems that include 1D porous media.

APPENDIX

The details of the derivation of Eq. (12):

$$\omega = \frac{D}{d}, \qquad \varepsilon = 1 - \frac{\pi dD}{4S}; \; Square \Rightarrow = \frac{\pi dD}{4(1-\varepsilon)}, \qquad \varphi = 1 - \varepsilon,$$

$$K = \frac{K}{dD} = 0.133 \frac{(S-d)}{dDS\sqrt{1-\varphi}}$$

$$\Rightarrow K = \frac{K}{dD} = 0.133 \frac{(S-d)}{dDS\sqrt{1-\phi}} = \frac{0.133}{\sqrt{1-\phi}}\left(\frac{-3d+3S-}{dDS}\right)$$

$$\Rightarrow K = \frac{0.133}{dD\sqrt{1-\phi}}(-3Sd + 3 - \frac{}{S})$$

$$\Rightarrow K = \frac{0.133}{dD\sqrt{1-\phi}}(\frac{\pi dD}{4(1-\varepsilon)} - 3\sqrt{(\frac{\pi dD}{4(1-\varepsilon)})} + 3 - \sqrt{(\frac{4(1-\varepsilon)}{\pi dD})})$$

$$\Rightarrow K = \frac{0.133}{\sqrt{1-\phi}}(\frac{\pi}{4(1-\varepsilon)} - 3\sqrt{(\frac{\pi}{4(1-\varepsilon)})} + 3\frac{d}{D} - \sqrt{(\frac{4(1-\varepsilon)}{\pi})})$$

$$\Rightarrow Eq.(12): K = \frac{0.133\left[\frac{\pi}{4\phi} - 3\sqrt{\frac{\pi}{4\omega\phi}} + \frac{3}{\omega} - \sqrt{\frac{4\phi}{\omega\pi}}\right]}{\sqrt{1-\phi}}$$

REFERENCES

[1]   Tomadakis M. M., Robertson T. J. , 2005, Viscous permeability of random fiber structures: comparison of electrical and diffusional estimates with experimental and analytical results, *Journal of Composite Materials* **39**(2): 163-188.

[2]   Gostick J. T., Fowler M. W., Pritzker M. D., Ioannidis M. A., Behra L. M. , 2006, In-plane and through-plane gas permeability of carbon fiber electrode backing layers, *Journal of Power Sources* **162**(1): 228-238.

[3]   Ismail M. S., Hughes K. J., Ingham D. B., Ma L., Pourkashanian M., 2012, Effects of anisotropic permeability and electrical conductivity of gas diffusion layers on the performance of proton exchange membrane fuel cells, *Applied Energy* **95**: 50-63.

[4]   Tamayol A., Hooman K., 2011, Thermal assessment of forced convection through metal foam heat exchangers, *Journal of Heat Transfer* **133**(11): 111801-111808.

[5]   Tamayol A., McGregor F., Bahrami M., 2012, Single phase through-plane permeability of carbon paper gas diffusion layers, *Journal of Power Sources* **204**: 94-99.

[6]   Kaviany M., 1995, *Principles of Heat Transfer in Porous Media*, Springer-Verlag, New York.

[7]   Yazdchi K., Luding S., 2012, Towards unified drag laws for inertial flow through fibrous materials, *Chemical Engineering Journal* **207–208**: 35-48.

[8]   Jackson G. W., James D. F., 1986, The permeability of fibrous porous media, *The Canadian Journal of Chemical Engineering* **64**(3): 364-374.

[9]   Tamayol A., Bahrami M., 2011, Transverse permeability of fibrous porous media, *Physical Review E* **83**(4): 046314.

[10]   Mattern K. J., Deen W. M. , 2008, Mixing rules for estimating the hydraulic permeability of fiber mixtures, *AIChE Journal* **54**(1): 32-41.

[11]   Happel J., 1959, Viscous flow relative to arrays of cylinders, *AIChE Journal* **5**(2): 174-177.

[12]   Carman P. C. , 1938, The determination of the specific surface of powders, *Journal of the Chemical Society, Transactions* **57**: 225-234.

[13]   Sullivan R. R., 1942, Specific surface measurements on compact bundles of parallel fibers, *Journal of Applied Physics* **13**(11): 725-730.

[14]   Sparrow E. M., Loeffler A. L., 1959, Longitudinal laminar flow between cylinders arranged in regular array, *AIChE Journal* **5**(3): 325-330.

[15]   Hasimoto H., 1959, On the periodic fundamental solutions of the Stokes equations and their application to viscous flow past a cubic array of spheres, *Journal of Fluid Mechanics* **5**(02): 317-328.

[16]   Kuwabara S., 1959, The forces experienced by randomly distributed parallel circular cylinders or spheres in a viscous flow at small Reynolds numbers, *Journal of the Physical Society of Japan* **14:** 527-532.

[17]   Sangani A. S., Acrivos A., 1982, Slow flow past periodic arrays of cylinders with application to heat transfer, *International Journal of Multiphase Flow* **8**(3): 193-206.

[18]   Drummond J. E., Tahir M. I., 1984, Laminar viscous flow through regular arrays of parallel solid cylinders, *International Journal of Multiphase Flow* **10**(5): 515-540.

[19]   Hellou M., Martinez J., El Yazidi M., 2004, Stokes flow through microstructural model of fibrous media, *Mechanics Research Communications* **31**(1): 97-103.

[20]   Tamayol A., Bahrami M., 2009, Analytical determination of viscous permeability of fibrous porous media, *International Journal of Heat and Mass Transfer* **52**(9): 2407-2414.

[21]   Gebart B. R., 1992, Permeability of unidirectional reinforcements for RTM, *Journal of Composite Materials* **26**(8): 1100-1133.

[22]   Van der Westhuizen J., Prieur Du Plessis J., 1996, An attempt to quantify fibre bed permeability utilizing the phase average Navier-Stokes equation, *Composites Part A: Applied Science and Manufacturing* **27**(4): 263-269.

[23]   Sahraoui M., Kaviany M., 1992, Slip and no-slip velocity boundary conditions at interface of porous, plain media, *International Journal of Heat and Mass Transfer* **35**(4): 927-943.

[24]   Sobera M. P., Kleijn C. R., 2006, Hydraulic permeability of ordered and disordered single-layer arrays of cylinders, *Physical Review E* **74**(3): 036301-036311.

[25]   Clague D. S., Phillips R. J., 1997, A numerical calculation of the hydraulic permeability of three-dimensional disordered fibrous media, *Physics of Fluids* **9**: 1562-1572.

[26]   Nabovati A., Llewellin E. W., Sousa A., 2009, A general model for the permeability of fibrous porous media based on fluid flow simulations using the lattice Boltzmann method, *Composites Part A: Applied Science and Manufacturing* **40**(6): 860-869.

[27]   Higdon J. J. L., Ford G. D., 1996, Permeability of three-dimensional models of fibrous porous media, *Journal of Fluid Mechanics* **308**: 341-361.

[28]   Dahua Sh., Lin Y., Youhong T., Jintu F., Feng D. , 2013, Transverse permeability determination of dual-scale fibrous materials, *International Journal of Heat and Mass Transfer* **58**(1–2): 532-539.

[29]   Dahua Sh., Lin Y., Jintu F., 2014, On the longitudinal permeability of aligned fiber arrays, *Journal of Composite Materials* 0021998314540192.

[30]   Xiaohu Y.,Tian Jian L., Tongbeum K., 2014, An analytical model for permeability of isotropic porous media, *Physics Letters A* **378**(30–31): 2308-2311.

[31]   Dahua Sh., Lin Y., Jintu F., 2015, Longitudinal permeability determination of dual-scale fibrous materials, *Composites Part A: Applied Science and Manufacturing* **68**: 42-46.

[32]   White F.M.,2003, *Fluid Mechanics*, McGraw-Hill Higher Education.

[33]   Archie G. E., 1942, The electrical resistivity log as an aid in determining some reservoir characteristics, *Transactions of the AIME* **146**(99): 54-62.

[34]   Shen L., Chen Z., 2007, Critical review of the impact of tortuosity on diffusion, *Chemical Engineering Science* **62**(14): 3748-3755.

[35]   Versteeg H. K., Malalasekera W., 1995, *An Introduction to Computational Fluid Dynamics*, Longman Scientific and Technical, Essex, UK.

[36]   Bergelin O. P., Brown G. A., Hull H. L., Sullivan F. W., 1950, Heat transfer and fluid friction during viscous flow across banks of tubes–III. A study of tube spacing and tube size, *Transactions of the ASME* **72**: 881-888.

[37]   Chmielewski C., Jayaraman K., 1992, The effect of polymer extensibility on crossflow of polymer solutions through cylinder arrays, *Journal of Rheology* **36**: 1105-1126.

[38]   Khomami B., Moreno L. D., 1997, Stability of viscoelastic flow around periodic arrays of cylinders, *Rheologica Acta* **36**(4): 367-383.

[39]   Kirsch A. A., Fuchs N. A., 1967, Studies on fibrous aerosol filters—II. Pressure drops in systems of parallel cylinders, *Annals of Occupational Hygiene* **10**(1): 23-30.

[40]   Sadiq T. A. K., Advani S. G., Parnas R. S., 1995, Experimental investigation of transverse flow through aligned cylinders, *International Journal of Multiphase Flow* **21**(5): 755-774.

[41]   Zhong W. H., Currie I. G., James D. F., 2006, Creeping flow through a model fibrous porous medium, *Experiments in Fluids* **40**(1): 119-126.

[42]   Skartsis L., Kardos J.L., 1992, The newtonian permeability and consolidation of oriented carbon fiber beds, *Proceedings of American Society of Composites Technical Conference* **5** :548-556.

[43]   Sangani A. S., Yao C. , 1988, Transport processes in random arrays of cylinders: II-viscous flow, *Physics of Fluids* **31**: 2435-2444.

[44]   Tamayol A., Bahrami M., 2010, Parallel flow through ordered: An analytical approach, *Journal of Fluids Engineering* **132**: 114502.